CFD lab, Test Case 2
Turbolent Water Transport In A Hydraulically Smooth Pipeline

Marta Pignatelli, Sofia Sannino

July 28, 2025

General Information

Report for the second test case of the Computational Fluid Dynamics laboratories within the course of Fluids Labs, by G. V. Messa, Politecnico di Milano.

1 Introduction

The case under observation is the turbulent water flow in a hydraulically smooth pipeline. The simulation will be taken using PHOENICS software and data will be post-processed through MATLAB.

2 Case description

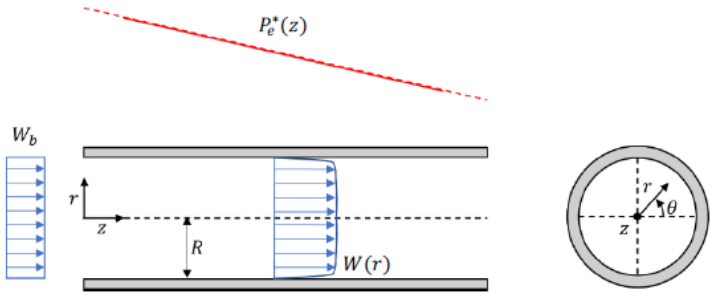

Figure 1: Sketch of the case

A uniform velocity profile is given as inflow, but, if the pipeline is long enough, one expects the flow to reach a fully developed state at a certain distance downstream of the left edge, and this must be reproduced by the CFD solution. Due to the intrinsic unsteadiness of the turbulent flow, all the considerations are made in a time-averaged context. Quantities of interest are the frictional losses along the pipeline, as well as radial profiles of axial velocity, shear stress (viscous and turbulent), and turbulent parameters. In the turbulent case, no analytical solution is available; therefore, no benchmarking is possible. Instead, experimental data and empirical correlations are used for validation of the numerical set-up, making a comparison with the PhD thesis by Lars Even Torbergsen (1998).

2.1 Numerical simulation

The Reynolds-Averaged Navier-Stokes(RANS) equations are solved, combined with the standard k-ε model. The problem will be simulated as 2D, through a domain having the shape of a circular sector, as shown in Figure 2, and hence it will be realized in PHOENICS by means of cylindrical

coordinates.
Objects to set the case:

- **Axisymmetry condition:** as default in such coordinates' system, it's exploited to reduce the computational burden of the simulations.
- **Inlet boundary condition:** a uniform z-velocity profile equal to W_b (bulk velocity) is imposed, whereas the r- and θ- velocity components are set to zero. No turbulence is assumed at the inlet: this is achieved by setting the turbulence intensity parameter TI to 0.
- **Outlet boundary condition:** at the outlet, a zero external P^* is imposed.
- **Wall condition:** walls are assumed to be fixed and a no-slip condition is set;
- **Null object:** to better evaluate the boundary conditions and set up a consistent grid independence study, we introduce a null object which divides the computational domain in two regions, each one with a different number of cells. In this way, we can create a region close to the wall with one line of cells of fixed size. Thus, when performing the grid independence study, the size of the nearest cell to the wall (size of y^+) remains invariable while the rest of the domain (number of cells) is modified.

To numerically solve and study the near-wall fluid turbulence, we adopt the wall function approach, using the equilibrium wall function of Lauder and Spalding (1974). On the one hand, the advection flux of variable W through the near-wall cell faces is set to zero. On the other hand, the diffusion flux of variable W through the near-wall cell faces (that is, the wall shear force) is specified by obtaining the wall shear stress from the equilibrium wall function of Launder and Spalding. Note that, since the wall function approach is adopted, the dimensionless wall distance y^+ of the first grid nodes must be greater than 30 (and generally lower than about 130). Such dimensionless wall distance y^+ can only be calculated a posteriori.

2.2 Configuration of the problem

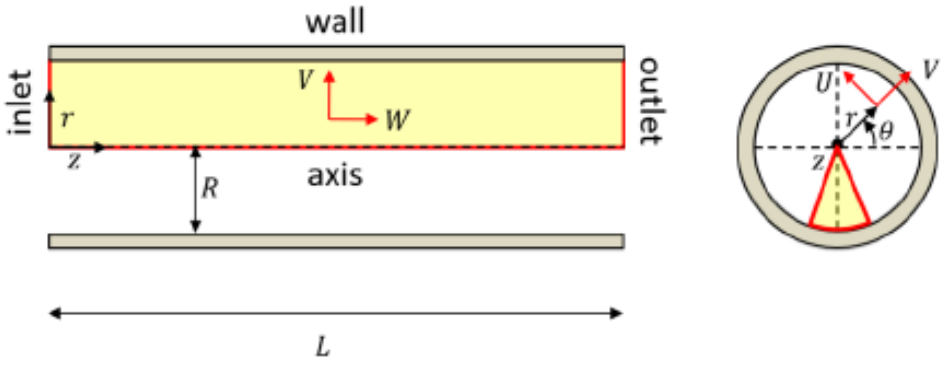

Figure 2: Domain and boundary conditions

Pipe diameter $2R = 0.10\ m$,
Bulk-mean velocity $W_b = 0.75\ m/s$,
Fluid = water at 20 °C, treated as incompressible
density $\rho = 998.23\ kg/m^3$
kinematic viscosity $\nu = 1.0 \times 10^{-6}\ m^2/s$

3 Analysis

3.1 Verify turbulence

To check the flow turbulence, we can simply compute the Reynolds bulk number $Re_b = DW_b/\nu$ related to the problem and verify whether it satisfies the rule $Re_b > 2000$.

$$Re_b = \frac{W_b \cdot D}{\nu} = 75000 > 2000$$

Indeed, the Reynolds number exceeds the critical threshold, so we are dealing with a turbulent flow.
Furthermore, we could verify the incompressibility of the fluid by computing the Mach number Ma and checking whether it satisfies $Ma < 0,3$. Unfortunately, Ma is defined as the ratio between a characteristic velocity of the problem, which could be W_b, and the velocity of sound in the fluid, which we are not given. We assume the fluid to be incompressible anyway, being simply water.

3.2 Study of domain length

The goal is to define a length that is sufficient to observe a fully developed flow. We recall that such state is characterized by:

$$\frac{\partial \phi}{\partial z} = 0 \quad \forall \phi \neq p_e$$

Moreover, we explicit that it's not our intention to optimize such length, and derive the so called *entry length* L_e, to reduce computational costs. However, since the simulations for this case start to be quite time demanding, we will be cautious when deciding the dimension of the domain and the refinement of the mesh.
As for the previous test case, for the sake of generality, we start by making use of dimensionless variables; hence we are going to rescale the lengths by dividing them by the radius of the pipe R. We remember that in the laminar case we chose a length that was 30 times larger than the radius of the pipe. Being in the turbulent case, it's reasonable to choose a longer pipe in order to study a fully developed flow, for example with a proportionality constant of $k = 100$, which corresponds to a $5m$ long pipe.
Then we set up the simulation, choosing a grid that is refined enough to be in the grid-independent region of the solution[1]. In table 1, there are shown the used grid parameters: note that the number of cells along the z-axis is proportional to the number of cells in the y direction, with a multiplicative coefficient of k, in order to get rather cubic cells. Additionally, a non-null power law option is set to get a non-uniform mesh: since the critical region should be near the wall, the refinement is higher there.

	#cells	power law
$x = \theta$	1[2]	none
$y = r$	15 + 1[3]	-1.25
z	1500	none

Table 1: Specifics of the chosen mesh.

Setting a maximum of 10000 iterations and a global convergence threshold of 10^{-3}, we obtain that the simulation converges in 3380 iterations and the fields look quite stable in the cell near the wall, at about 90% of the length, where the probe is put (see Figure 3).

[1] We will see in the paragraph 3.4 whether we can accept these results.
[3] This is intended to obtain a 2D simulation.
[3] The near-wall cells are divided from all others by the *null object*.

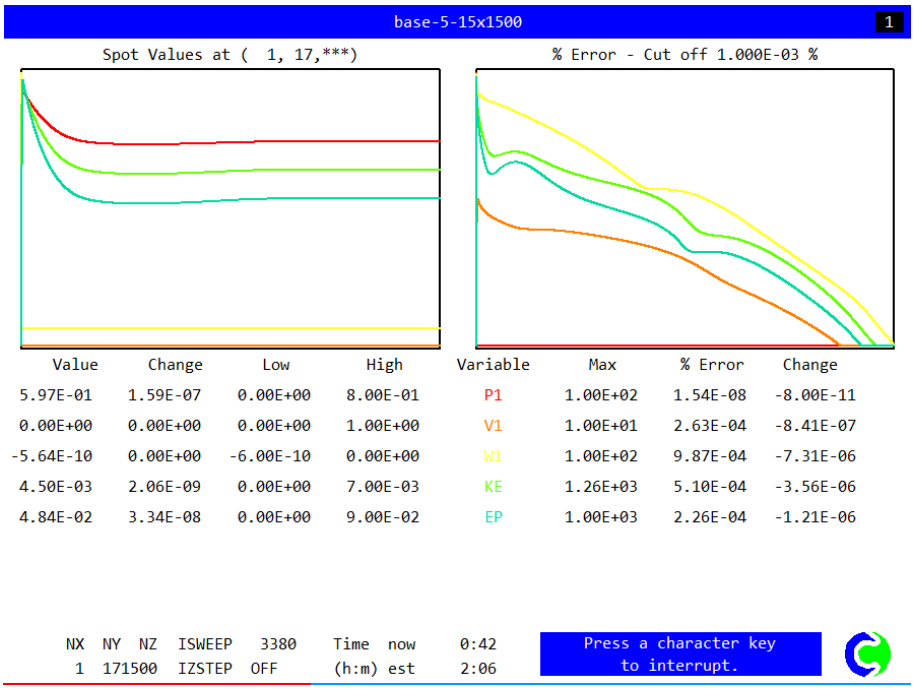

Figure 3: Spot values and residuals

First of all, we check that the solution is acceptable from the point of view of the turbulence model (standard $k-\varepsilon$): it is indeed, given that the values of y^+ stay in the range $(89, 112)$, so $30 < y^+ < 130$, thanks to the null object positioning at $0.045m = 90\%R$ from the centerline. Then, we inspect the colour plots of pressure and velocity:

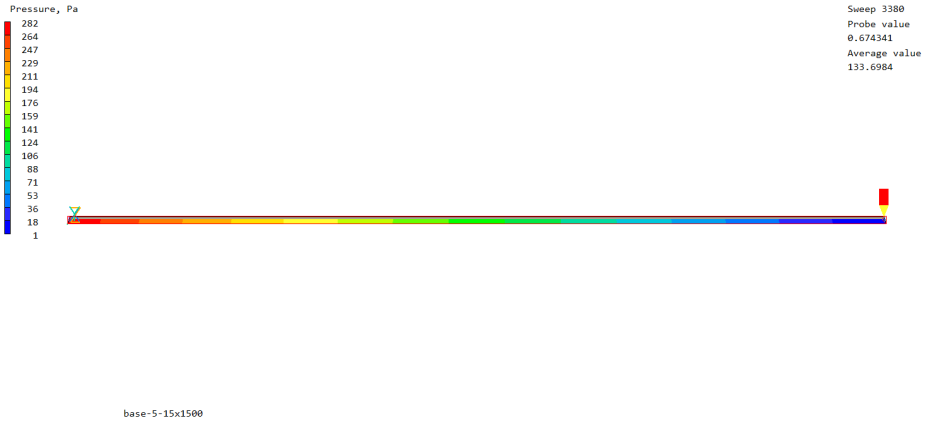

Figure 4: Pressure field

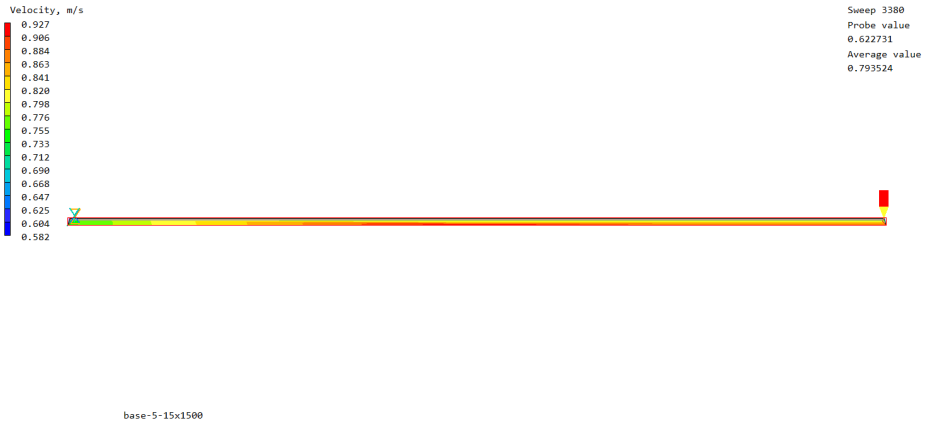

Figure 5: Velocity

Qualitatively, both fields seem physically sound. In particular, the pressure seems rather homogeneously descending in the last part of the pipe. The velocity may seem to be invariate from about 80% of the domain onward: that is the portion of tube where we could assume the flow to be fully developed.
To confirm such hypothesis, applying a quantitative criterion is necessary. We decide to look at the values of $\frac{\partial w}{\partial z}$, saved from the PHOENICS environment, along the z-axis, both near the centre of the cylinder, where velocity reaches its maximum value, at a mid distance between the centre and the wall, and near the edge, where velocity patterns should be more interesting. We state that fully developed state is obtained if such derivatives go below the arbitrary threshold of 1% .
We process the data in MATLAB and we get that, starting from the 1236^{th} cell, so about 85% of length downstream of the inlet (which corresponds to $k \cdot 0.85 = 85$ times the radius of the pipe), the flow stabilizes (it satisfies our chosen criterion) in each of the cells. See Figure 6.

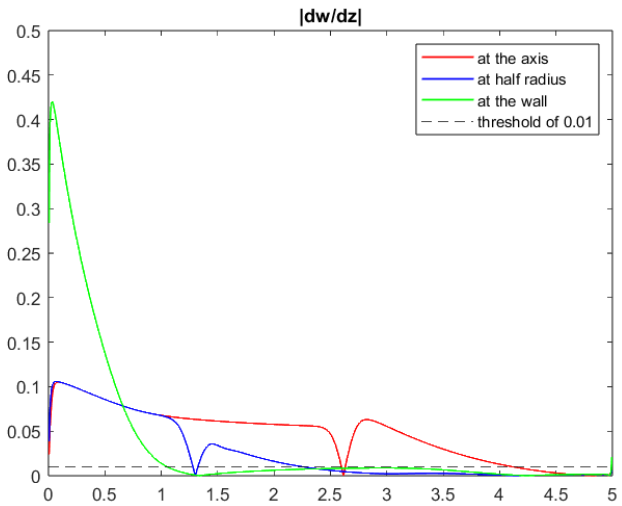

Figure 6: Plot of $|\frac{\partial w}{\partial z}|$

In comparison with the laminar case, we can observe that the trend of the derivative is not monotone here, it declines overall, but it presents some not fully understood drops and rebounds. Given this, we ensure that the fully developed region is where the criteria is satisfied by all the cells, and we avoid taking as region the cells after the first ones that satisfy the condition (which

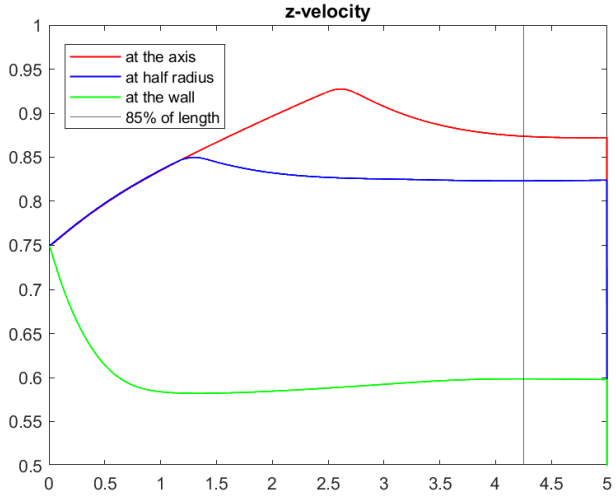

Figure 7: z-velocity at different y values

would be all cells after one of the sudden dips and that would be wrong). Investigating these oscillations, it seems that the singularity repeats itself, happening first in the centre line and then propagating toward the wall, further in the length of the tube: this may exhibit the transport of turbulence.

One more thing to notice is that, as expected, the near wall region is the first to stabilize around zero[4] (adapting to the no-slip condition), thanks to viscous effects, while going towards the centre it takes more space for the velocity to get flat and its value remains higher (as it should). Finally, the velocity goes to zero[5] in the very last cells because of automatic 'in cell' zero value in the outlet condition.

Entrance lengths L_e found in the literature are various and mostly qualitative; we point out just some of them:

- The most widely used empirical formula [1], whose author is not precisely definite, is $\frac{L_e}{R} \simeq 2 \cdot 4.4\ Re^{\frac{1}{6}} \simeq 57.15$, which is way less strict than the one we found;
- A more precise correlation was given by recent studies of F. Anselmet and S. Dash [1] and it's $\frac{L_e}{R} \simeq 2 \cdot 1.6\ Re^{\frac{1}{4}} \simeq 52.96$, even further from ours;
- From [2], we can read a similar estimate: $\frac{L_e}{R} \simeq 2 \cdot 1.359\ Re^{\frac{1}{6}}$, but it's also mentioned that in most practical engineering applications the length is approximated to be about $10 \cdot 2R$, still much under our result;
- Nikuradse [3] proposes an entrance length of $40 \cdot 2R$, and this is the estimate most similar to ours;
- Lien et al. [4] recommended instead $L_e \simeq 150 \cdot 2R$: this value is much higher than our guess, and we've also found that it refers to very high Reynold numbers, in particular, greater than 10000, which is the case.

Surprisingly for us, one thing that most of these books and sites report is that the approximation of entry length for turbulent flow is much shorter than in the case of laminar flow. This does not correspond to our result, since we found that in laminar flow about 27 times the radius is enough to get a fully developed flow, while for turbulent flow, a length around 85 times the radius is necessary.

[4]Remember that the velocity is evaluated at a certain distance from the wall, which is half the height of the last row of cells.

[5]Note that the plot is zoomed.

3.3 Solution inspection

In order to evaluate the quality of our CFD simulation we start by checking qualitatively our solution, so we inspect the colour plots of pressure and velocity, reported in Figure 4 and Figure 5. They appear to be fine, showing no weird patterns; the variables behave as one would expect. Another thing to put attention to is the velocity in the y-direction (r-direction): as it should be, it is (almost) null from about half of the domain onwards (see Figure 8 below). With respect to the laminar case, it exhibits higher values in the first part of the pipe, indicating that the flow is in fact more chaotic.

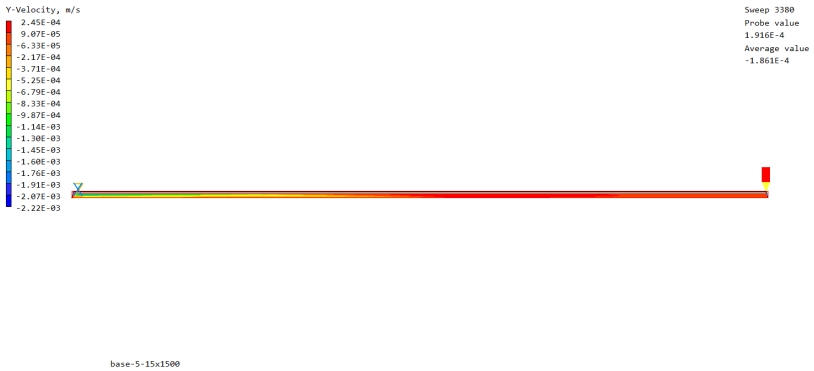

Figure 8: Colour plot of r-velocity

Furthermore, to verify that the solution is physically sound, we check the pressure behaviour as a function of the z-coordinate. It is in our interest to show how it evolves along the centerline and near the wall, parallel to the z-axis. As shown in Figure 9, it is nice to note that, indeed, the pressure decreases linearly in the (supposed) fully developed region, as it should be according to theoretical estimates.

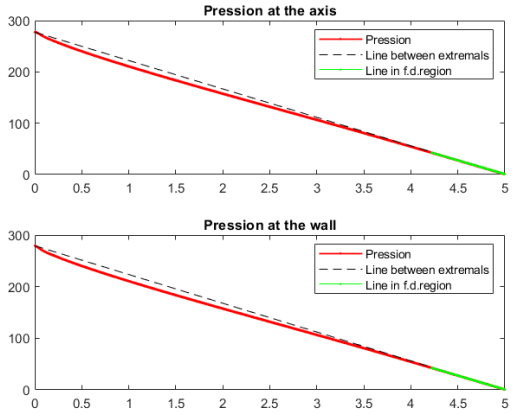

Figure 9: Pressure profile

It can be useful to check as well the profile of the Reynolds average velocity along the pipe radius, which can be expressed in the two following dimensionless forms:

- W/W_b versus r/R, where R is the pipe radius.
- w^+ versus y^+, where $y^+ = yw_\tau/\nu$, $w_\tau = \sqrt{\tau_w/\rho}$ is the friction velocity and y the distance from the pipe wall ($y = R - r$).

Evaluating the first plot, we can see that the experimental results match the theoretical expectations. Indeed, we know that the velocity profile versus r usually follows the Power Law Profile of Nikuradse (see validation): $W(r) = W(r = 0) \cdot (1 - r/R)^{\frac{1}{n}}$ The experimental plot is shown in Fig. 10.

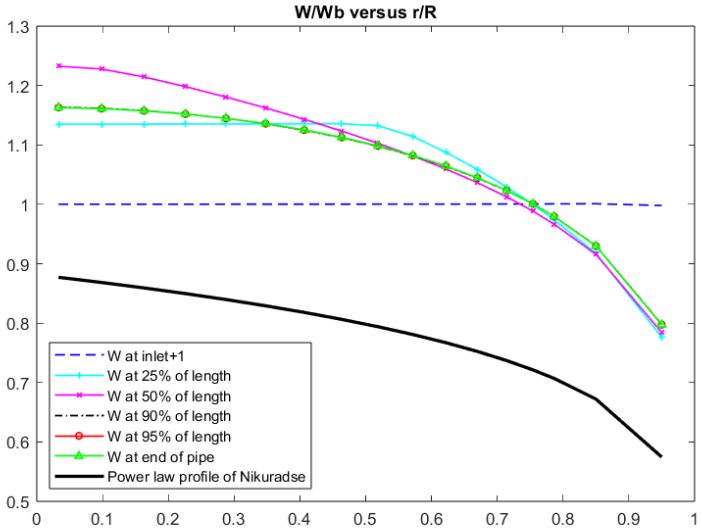

Figure 10: W/Wb versus r/R

In the same way, we observe that also the second plot follows the theoretical expectations. y^+ represents the cell center distance, in wall units, from the wall and it is crucial to evaluate if our simulation models correctly the flow near the borders. We intend to apply the **wall function model** to study the flow near the walls. In order for this model to work correctly, it needs y^+ in $[30, 130]$. In this case, $y+$ follows the **Log Law**, since the mentioned y^+ values are in the inner layer. Our first simulation showed values of y^+ below 30, so we increased the value of the separated null object region, so the near-wall cells could have a longer distance in wall units from the wall. With the second simulation, the plots obtained can be observed in Figures 11a and 11b. In the first log-log plot, we can perfectly see that $w^+ = w^+(y^+)$ follows a logarithmic pattern. To be more precise, $w^+ = w^+(y^+)$ should behave as the Log Law: $w^+ = \frac{1}{K} log(y^+) + B$. Indeed, in the second figure, w^+ follows the Log Law up to multiplicative constants (see validation).

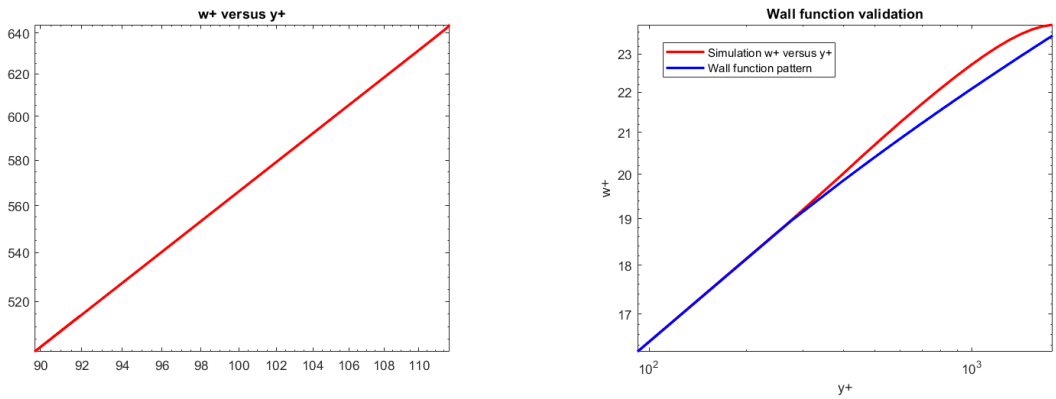

(a) W/Wb versus r/R

(b) $\frac{W}{w_\tau}$ versus $\frac{(R-r)w_\tau}{\nu}$

Figure 11

Moreover, being in a turbulent flow context, it is important to study the shear stress behaviour. We know from the theory that:

$$\tau(r) = \tau_{viscous} + \tau_{Reynolds} = \mu \frac{dW}{dr} - \rho < u'v' > \approx \mu \frac{dW}{dr} + \mu_{turb} \frac{dW}{dr}$$

We understand from the theoretical model that $\mu_{turbulent} = \rho C_\mu \frac{k^2}{\varepsilon}$. Calculating both the shear stress components using $DWDY = \frac{dW}{dy}$, $KE = k$, $EP = \varepsilon$ and τ_{wall} from $STRS = \tau/\rho$, we obtain the following a-dimensional plots.

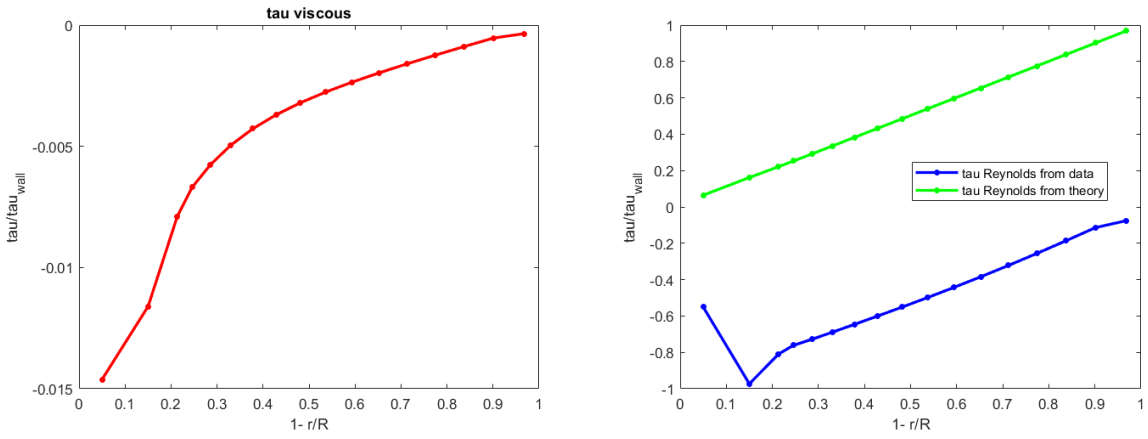

(a) $\tau_{viscous}$ (b) $\tau_{Reynolds}$

Figure 12

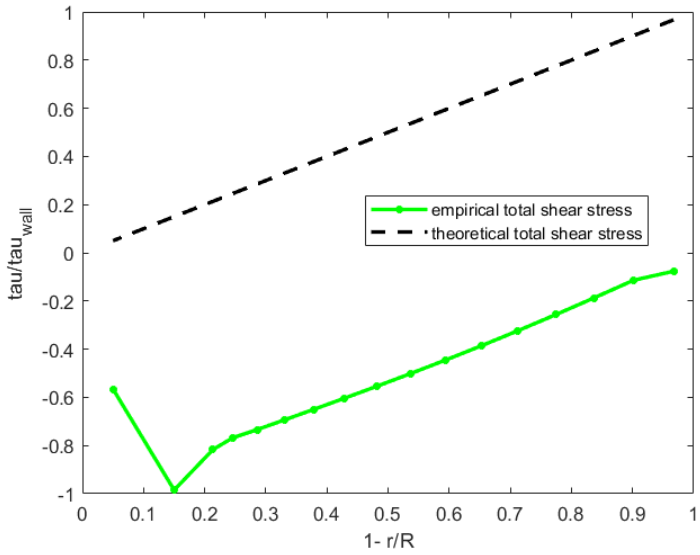

Figure 13: τ_{total}

We can observe that according to theory, $\tau_{viscous}$ is negligible far from the wall, while it is the main stress component in the borders; at the same time, $\tau_{Reynolds}$ has very high values near the center of the pipe, decreasing until it is negligible at the wall. It is useful to note that $\tau_{Reynolds}$ pattern follows the expectations: indeed, the theoretical line represents $(1 - \frac{r}{R}) - \frac{\tau_{viscous}}{\tau_{wall}}$. The last plot shows $\tau_{total} = \tau_{viscous} + \tau_{Reynolds}$, where x and y coordinates are respectively normalized

by R and τ_{wall}: even in this case we can observe that the total shear stress follows the theoretical pattern, $(1-\frac{r}{R})$. Since $DWDY$ is negative everywhere, we have negative shear stress values.

Other quantities of interest are:

- the profile of the turbulent kinetic energy, k, along the pipe radius, presented in dimensionless form as k/W_b^2 versus r/R
- the profile of the turbulent dissipation rate, ϵ, along the pipe radius, presented in dimensionless form as ϵ/W_b^3 versus r/R

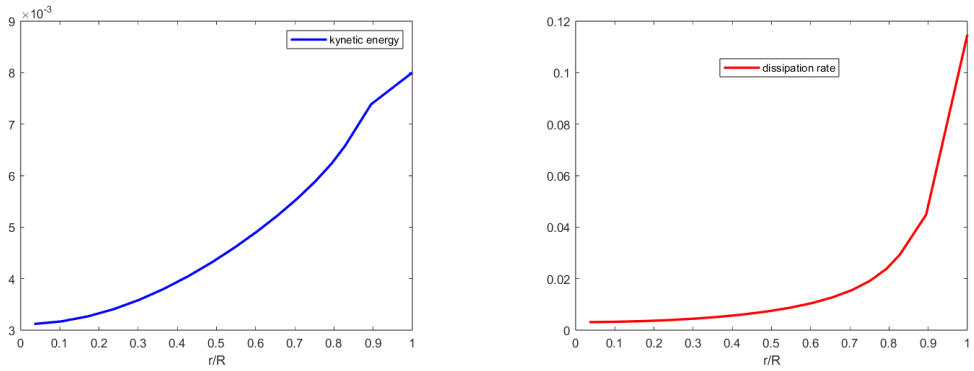

(a) Adimensional kinetic energy (b) Adimensional dissipation rate

Figure 14

Referring to Figure 14, we don't have much of theoretical ground to analyze these measures, however, one could say that they are physically plausible:

- About k:
  - it is small at the centre due to low shear;
  - it increases toward the wall where velocity gradients (and thus turbulence production) increase;
  - the increase is mild;
  - we could not see the vanishing of k at the wall (where the velocity, and hence velocity fluctuations, go to zero) because our nearest cell to the wall is still too far from the boundary.
- About ε:
  - it is low in the core of the pipe;
  - it rises steeply going to the wall, which it's okay because ε depends on the gradient of the velocity fluctuations, which enlarge approaching the wall.

3.4 Numerical convergence

- Convergence of simulation
  As one can detect from figure 3, the simulation achieves convergence in 3380 iterations, it does not display oscillations, and the whole-field residuals constantly reduce towards the chosen threshold, even if their decrease velocity reduces at about half of the simulation.

- Grid independence study
  The target parameters of the grid independence study are W, $\frac{\partial W}{\partial y}$, P, k and ε. In table 2 are reported the meshes on which the study has been carried out. In each of them, the distribution of the cells is not uniform, but it follows a power law of -1.25 along the radius direction, such that the more critical wall region is resolved in a finer way, except for the last line of cells, which has fixed height of 0.005m in order to get an acceptable value of y^+ for the turbulence model.
  The method adopted consists of comparing the reference mesh (the one used for all previous sections) with a coarser grid and a finer one. These two are constructed refining only along the y-direction, since the last test case taught us that along the axis of the pipe refinement is not relevant.

ID	# cells	$x = \theta$	$y = r$	z
coarse	16500	1	10+1	1500
base	24000	1	15+1	1500
refined	31500	1	20+1	1500

Table 2: Parameters of the meshes for the grid independence study

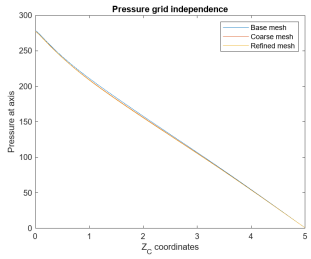

(a) Pressure

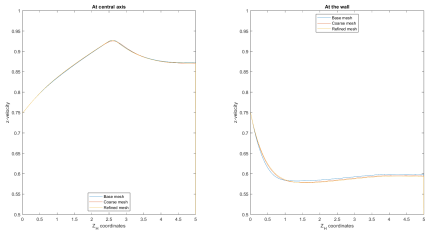

(b) z-velocity

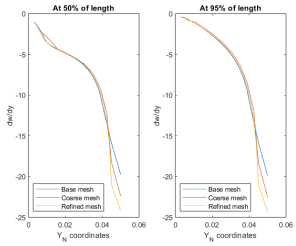

(c) $\frac{\partial W}{\partial y}$

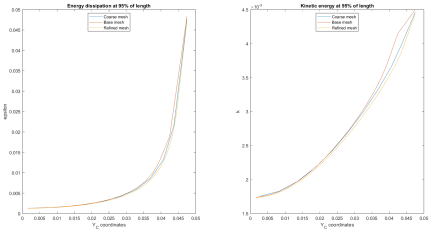

(d) k and ε plot along radius at $z = 0.95\ L$

Figure 15: Grid independence plots

The results are satisfying: as shown in Figure 15, each variable looks grid independent, since the graphs almost overlap. Quantitatively, we've computed the area under each curve through the MATLAB function *trapz* and we've evaluated the relative difference of the integrals between different meshes: all stay under a 2% variation, leading us to accept the assumption of grid independence[6].

[6]If increasing the refinement gets a decrease in the relative difference, this indicates convergence.

3.5 Validation

Since no analytical solution is available in the turbulent case, the CFD results are compared against experimental data and some empirical formulas available in the literature. Specifically, the experimental data originate from the PhD thesis by **Lars Even Torbergsen (1998)**, who investigated the fully developed air pipe flow at a Reynolds number similar to the one of the present test case. The scope of the comparison against reference data is two-fold. On the one hand, it can be used to check that a proper selection of the modeling settings (here, the turbulence model) has been made. On the other hand, it can be used to decide the most appropriate modeling settings, e.g., the best turbulence model within a given set of options. Now we would like to prove the validation of the model used.

3.5.1 Frictional losses

We firstly inspect the frictional losses, which are quantified through the friction coefficient f [7]. We will calculate the friction factor obtained from the CFD simulation, f_{CFD}, by means of the Darcy-Weisbach formula, taking two points in the fully developed region:

$$f_{CFD} = -\frac{2\Delta P \cdot D}{\rho \cdot L \cdot W_b^2} = 0.0192$$

Then, we will compare it against:

- Data obtained experimentally by Torbergsen;
- Moody chart (graphic estimate);
- Formula by Prandtl for hydraulically smooth pipes;
- Formula by Haaland for hydraulically smooth pipes.

Torgbersen (1998) data The friction factor derived by Torbergsen is equal to 0.0190, hence the relative difference between it and our result is $\frac{|f_{Tor} - f_{CFD}|}{f_{Tor}} = 0.0131 \simeq 1\%$.

Moody chart (graphic estimate) For reference, we report the Moody chart in Figure 16.

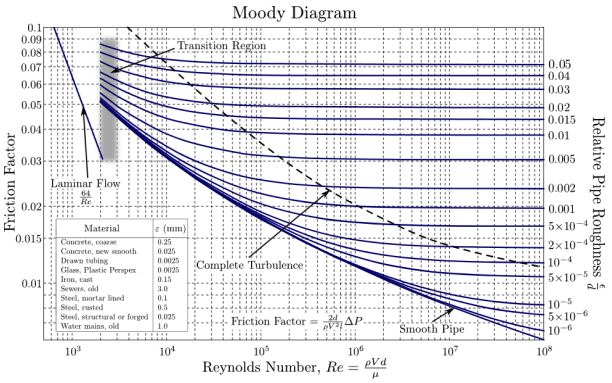

Figure 16: Moody chart

Given that $Re_b = 75000$, looking at the graph for $s = 0$ we can see that approximately f has a value of 0.0190, still very close to the values above.

[7] Studying this parameter is equivalent to look at the skin friction coefficient C_f, the hydraulic gradient J, the pressure gradient $-\frac{dP^*}{dz}$ or the wall shear stress τ_w, since they are all related to frictional losses

Formula by Prandtl for hydraulically smooth pipes The formula given by Prandtl is:

$$\frac{1}{\sqrt{f}} = -2\ log_{10}(\frac{2.51}{Re_b\sqrt{f}})$$

To obtain the value of f, which is implicit in the expression, we exploit the Newton algorithm and we get: $f \simeq 0.0191186$.

Formula by Haaland for hydraulically smooth pipes The formula given by Haaland is:

$$\frac{1}{\sqrt{f}} = -1.8\ log_{10}(\frac{6.9}{Re_b}) \Rightarrow f = \left[-1.8 \log_{10}\left(\frac{6.9}{Re_b}\right)\right]^{-2} = 0.0189455$$

This value is a little bit more distant from the others but id doesn't exceed a relative variation of 2% (it is indeed 0,0134).

In conclusion, the frictional losses obtained with our CFD simulation are compatible with the ones we compared them to and validate our result.

3.5.2 Profile of the Reynolds-averaged axial velocity along the pipe radius

We carry out the Reynolds averaged axial velocity validation, comparing our results in three ways:

- Data obtained experimentally by Torbergsen;
- Power law profile of Nikuradse;
- Wall function by Launder and Spaulding.

Data obtained experimentally by Torbergsen(1998) We would like to confront our Reynolds-averaged axial velocity values with the experimental data obtained by Torbergsen. Two data series are provided, containing each $\frac{W}{W_b}$ versus $\frac{r}{R}$ obtained with two different post-processing operations. We can observe the comparison between our simulation data and the two different data series in Fig. 17 and note that they follow the same pattern. We can conclude that our experiment validation outcome is, in this case, positive.

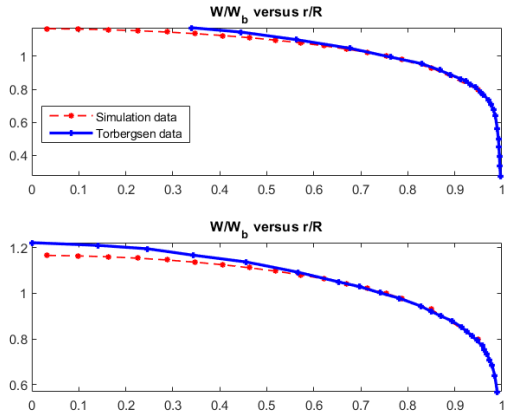

Figure 17: Comparison between Torbergsen Reynolds-averaged axial velocity and simulation data

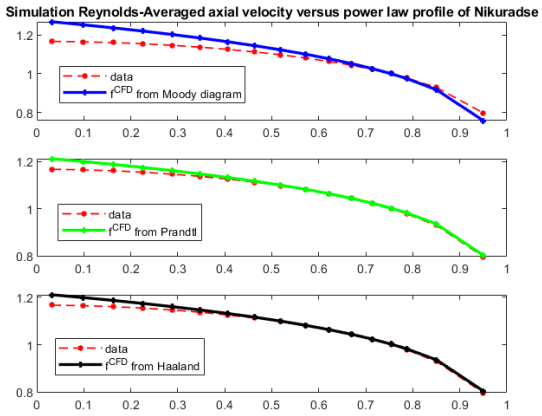

Figure 18: Comparison between Nikuradse's Profile Law averaged axial velocity and simulation data

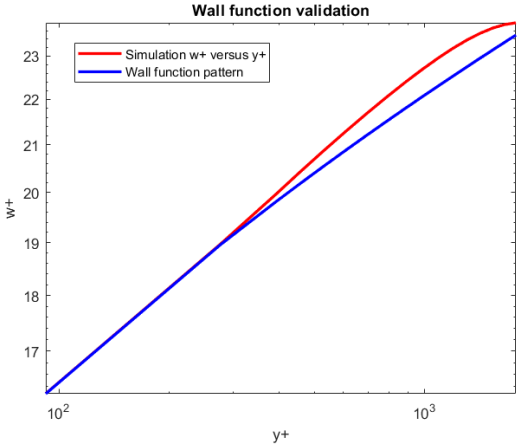

Figure 19: $\frac{W}{w_\tau}$ versus $\frac{(R-r)w_\tau}{\nu}$

Power law profile of Nikuradse As a second validation step for our simulation Reynolds-averaged axial velocity, we would like to take as benchmark the power law profile of Nikuradse, normalized by the bulk velocity W_b: $\frac{W}{W_b} = \frac{(2n+1)(n+1)}{2n^2}(1-\frac{r}{R})^{\frac{1}{n}}$ where $n = f_{CFD}^{-0.5}$ and f_{CFD} is the friction factor. We calculate the friction factor in three ways: through Moody diagram ($f_{CFD} = 0.019$), through Prandtl's formula $\frac{1}{\sqrt{f}} = -2\log_{10}\left(\frac{2.51}{Re\sqrt{f}}\right)$ ($f_{CFD} = 0.0191$) and through Haaland's formula $\frac{1}{\sqrt{f}} = -1.8\log_{10}(\frac{6.9}{Re})$ ($f_{CFD} = 0.0189$). As we can observe in Fig. 18, where we plot W/W_b versus r/R using our data and Nikuradse's profile, simulation results are consistent with the Nikuradse's profile and the most accurate friction factor is calculated through Prandtl and Haaland.

Wall function by Launder and Spaulding The wall function of Launder and Spalding (1974) for hydraulically smooth pipes, expressed in dimensionless form as y^+ versus w^+, reads as follows: $w^+ = \begin{cases} y^+ & \text{if } w^+ < 11.6 \\ \frac{1}{41}log(8.2w^+) & \text{if } 11.6 \leq w^+ < 130 \end{cases}$
We would compare the pattern of y^+ versus w^+ calculated through our numerical simulation to the theoretical expectations just exposed. As we show in Fig. 19, the two loglog-plots are almost overlapping.

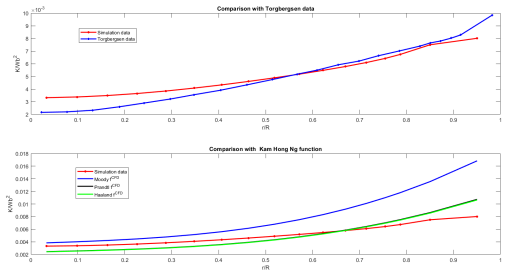

Figure 20: $\frac{k}{W_b^2}$ versus $\frac{r}{R}$

3.5.3 Profile of the turbulent kinetic energy along the pipe radius

Then, the validation is extended to the profile of the turbulent kinetic energy along the pipe radius. We present the results in dimensionless form as k/W_b^2 versus r/R. The terms of comparison are as follows:

- Torgbersen (1998) data;
- Kam Hong Ng (1971) empirical formula, presented in dimensionless form.

Torgbersen (1998) data We would like to confront our kinetic energy values with the experimental data obtained by Torbergsen (1998). A data series is provided, containing $\frac{k}{W_b^2}$ versus $\frac{r}{R}$. We can observe the comparison between our simulation data and the two different data series in Fig. 20 and note that, although they exhibit a similar overall trend, there are substantial differences: this validates our model, since the pattern is reasonable with respect to a similar experiment like the Torbergsen one.

Kam Hong Ng (1971) empirical formula Kam Hong Ng in his/her PhD thesis obtained the following empirical formula, that models the $\frac{k}{W_b^2}$ versus $\frac{r}{R}$ behavior:

$$\frac{k}{W_{\text{bulk}}^2} = \frac{f^{CFD}}{8}(1 + \frac{2}{3}\frac{r}{R} + \frac{10}{3}(\frac{r}{R})^3)$$

We want to compare the simulation $\frac{k}{W_b^2}$ versus $\frac{r}{R}$ pattern with the one we obtain through the just mentioned formula: we show the results in Fig. 20, with friction factor calculated respectively with Moody chart, Prandtl's formula and Haaland's formula. As we can see, the the trend is very similar to the Kam Hong Ng function one, especially in the Prandtl and Haaland case.

3.5.4 Profile of the turbulent dissipation rate along the pipe radius

Finally, the validation is focused on the profile of the turbulent dissipation rate ϵ. We present the results in dimensionless form as $\frac{\epsilon R}{W_b^3}$ versus $\frac{r}{R}$. The terms of comparison are as follows:

- Torbergsen (1998) data;
- Relationship between k and ϵ in the $k-\epsilon$ model.

Torbergsen (1998) data We want to confront simulation dissipation rate values with data obtained experimentally by Torbergsen (1998), already presented in dimensionless form $\frac{\epsilon R}{W_b^3}$ versus $\frac{r}{R}$. Specifically, three data series are provided, which correspond to different methods for estimating ϵ from the same experimental data point. We obtain the results showed in Fig. 21 :

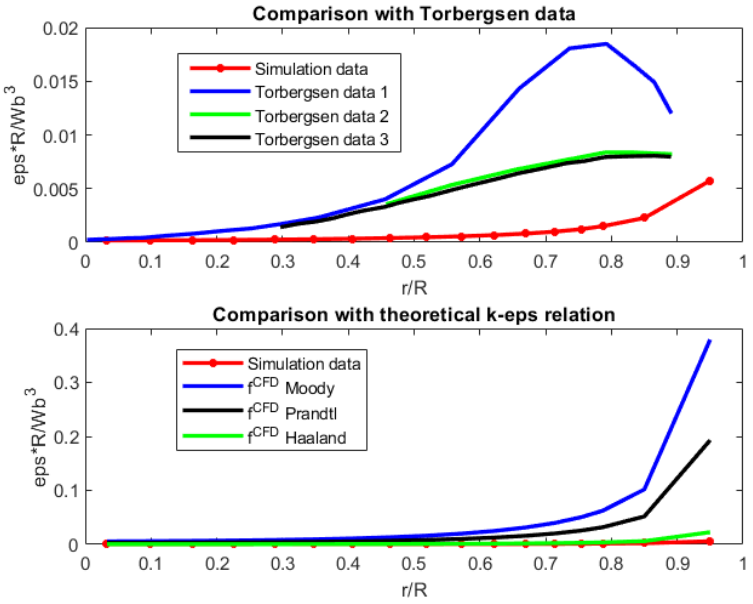

Figure 21: $\frac{\epsilon R}{W_b^3}$ versus $\frac{r}{R}$

unfortunately, our trend is radically different from the Torbergsen one, so it could be useful to validate our model with a different benchmark.

Relationship between k and ϵ in the $k-\epsilon$ model Finally, we would like to validate our ϵ values with a foundational relation between k and ϵ in the standard $k-\epsilon$ model: $\epsilon(r) = Cd\frac{k(r)^{3/2}}{lm(r)}$, where lm is the mixing length, calculated through the following empirical distribution by Nikuradse: $lm(r) = R(0.14 - 0.08(\frac{r}{R})^2 - 0.06(\frac{r}{R})^4)$. k can be calculated as well using the cubic correlation by Kam Hong Ng (1972) presented before. The result are shown in Fig. 21 and we note that the dissipation rate is the same, in particular ϵ obtained with Haaland friction factor almost overlaps with our data.

References

[1] EngineerExcel. Entrance length in pipe systems: Understanding factors and calculations.

[2] Y.A. Çengel and J.M. Cimbala. *Fluid Mechanics: Fundamentals and Applications*. McGraw-Hill Education, 2018.

[3] Johann Nikuradse. Gesetzmäßigkeiten der turbulenten strömung in glatten rohren. *Forschung auf dem Gebiet des Ingenieurwesens*, 3:1–36, 1932. Translated as NASA TT F-10,359, 1966.

[4] Kim Lien, Jason Monty, Michelle Chong, and Andrew Ooi. The entrance length for fully developed turbulent channel flow. 01 2004.